Crystal Structure of HIV-1 Reverse Transcriptase Bound to a Non-Nucleoside Inhibitor with a Novel Mechanism of Action

ARTICLE *in* ANGEWANDTE CHEMIE INTERNATIONAL EDITION · MARCH 2010

Impact Factor: 11.26 · DOI: 10.1002/anie.200905651 · Source: PubMed

Structural Biology

DOI: 10.1002/anie.200905651

Crystal Structure of HIV-1 Reverse Transcriptase Bound to a Non-Nucleoside Inhibitor with a Novel Mechanism of Action**

Séverine Freisz, Guillaume Bec, Marco Radi, Philippe Wolff, Emmanuele Crespan, Lucilla Angeli, Philippe Dumas, Giovanni Maga, Maurizio Botta, and Eric Ennifar**

HIV-1 reverse transcriptase (RT) is a heterodimeric enzyme that converts the genomic viral RNA into proviral DNA. HIV-1 RT inhibitors used in antiretroviral therapy are divided into two classes: 1) nucleoside-analogue RT inhibitors (NRTIs), which compete with the natural nucleoside substrate and terminate proviral DNA synthesis, and 2) non-nucleoside RT inhibitors (NNRTIs), which are a family of structurally diverse compounds that bind to a hydrophobic pocket (non-nucleoside inhibitor binding pocket, NNIBP) adjacent to the polymerase active site. In spite of the efficiency of NRTIs and NNRTIs, the rapid emergence of multidrug-resistant mutations requires the development of new RT inhibitors with an alternative mechanism of action.

Recently, two families of compounds forming a new class of HIV-1 RT inhibitors with a novel inhibition mechanism have been reported: the indolopyridones VRX-329747[1] and INDOPY-1 (or VRX-413638),[1–3] and the 4-dimethylamino-6-vinylpyrimidines[4,5] (DAVPs, Scheme 1). Unlike classical NNRTIs, these non-nucleoside RT inhibitors compete with the nucleotide substrate and remain unaffected by most mutations that alter NNRTIs binding and activity.[1–5] Consequently, it was proposed to refer to this class of compounds as "nucleotide-competing RT inhibitors" (NcRTIs).[2,6] In contrast to common NNRTIs, the antiviral activity of INDOPY-1 is not restricted to HIV-1 but is extended to HIV-2 and SIV,[3] likely reflecting the binding of the inhibitor close to the polymerase active site.[1,3] Unfortunately, attempts to obtain a crystal structure of the RT/INDOPY-1 complex were unsuccessful, probably because of the specificity of this NcRTI for the RT/template primer complex.[1]

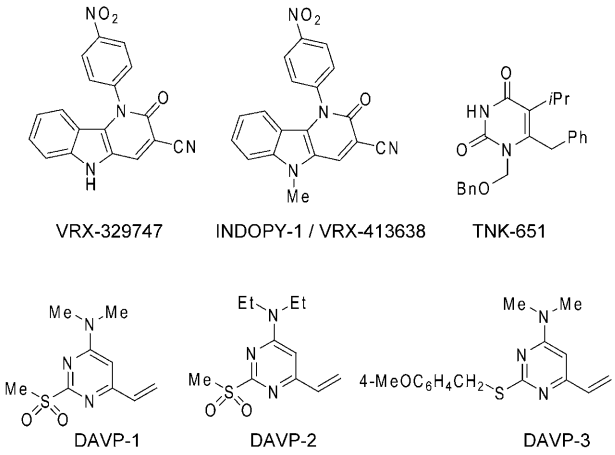

Scheme 1. Chemical structures of the DAVP derivatives, the reference NNRTI (TNK-651), and the indolopyridones VRX-329747 and INDOPY-1.

Here we present the first crystal structure at 2.5 Å resolution of the HIV-1 RT bound to a NcRTI, DAVP-1. The structure reveals a novel binding site, distinct from the NNIBP and close to the RT polymerase catalytic site. The structural requirements for binding of this NcRTI to the RT disclosed by this structure provide essential information for the rational development of new NcRTIs.

Because of their structural similarity with the non-nucleosidic reference compound TNK-651[7] (Scheme 1) and the loss of activity observed against the two most frequent mutations associated with NNRTIs resistance (Lys103Asn and Tyr181Ile), it was initially expected that the DAVPs would also behave as NNRTIs.[4] However, enzymological studies on DAVP-1, DAVP-2, and DAVP-3 revealed a competitive inhibition mechanism with the nucleotide substrate, similar that of the indolopyridone INDOPY-1. But in contrast to INDOPY-1, the binding kinetics of DAVP-1 did not indicate a specificity for the RT/template primer complex: kinetic analysis revealed that DAVP-1 binds the free RT with the same equilibrium dissociation constant as the RT/DNA complex ($K_i = 8$ nM).[5] In addition, a marked decrease of the association rate (k_{on}) was observed only for the RT/DNA/dNTP complex (compared to the free enzyme and to the RT/DNA complex), with no significant change in the dissociation rate (k_{off}). These data are therefore consistent with the classification of DAVP-1 in the newly identified NcRTI class of RT inhibitors.[6] Considering the peculiar behavior of this

[*] S. Freisz, Dr. G. Bec, P. Wolff, Dr. P. Dumas, Dr. E. Ennifar
Architecture et réactivité de l'ARN, Université de Strasbourg
CNRS, Institut de Biologie Moléculaire et Cellulaire
15 rue René Descartes, 67084 Strasbourg (France)
E-mail: e.ennifar@ibmc.u-strasbg.fr
Homepage: http://www-ibmc.u-strasbg.fr/arn/Dumas/index_dum_en.html
Dr. M. Radi, Dr. L. Angeli, Prof. M. Botta
Dipartimento Farmaco Chimico Tecnologico, University of Siena
Via Alcide de Gasperi 2, 53100 Siena (Italy)
E-mail: botta@unisi.it
Dr. E. Crespan, Dr. G. Maga
Istituto di Genetica Molecolare, IGM-CNR
Via Abbiategrasso 207, 27100 Pavia (Italy)

[**] We thank V. Olieric for his support at the SLS synchrotron. This work was supported by grants from the Agence Nationale de Recherche sur le SIDA (ANRS) to E.E. and from the European TRIoH Consortium (LSHB-2003-503480) to M.B. and G.M. E.C. is the recipient of a FIRC fellowship. M.B. thanks William L. Jorgensen and Karen S. Anderson for helpful discussions.

Supporting information for this article is available on the WWW under http://dx.doi.org/10.1002/anie.200905651.

compound, we attempted to solve the crystal structure of the RT/DAVP-1 complex to provide structural insights into the NcRTI binding site on the apo-RT.

Prior to our crystallization experiments, the binding of DAVP-1 to the free RT in the crystallization buffer was confirmed using mass spectrometry. Co-crystallization of the RT/DAVP-1 complex led to two crystal forms, both differing from previously reported RT crystal structures. The two crystal forms showed a nearly identical structure (root mean square deviation, rmsd = 0.72 Å) of the enzyme (see the Supporting Information). A first striking feature of this structure is that it reveals a new binding site on the RT: unlike NNRTIs, DAVP-1 does not bind the NNIBP, but rather in a hinge region at the interface between p66 thumb and palm subdomains (see Figure 1 and the Supporting Information), in the vicinity of the nucleotide binding site[8] and close to the polymerization catalytic site targeted by NRTIs. There are interactions with several residues essential for nucleic acid recognition (inset in Figure 1; primary contacts are detailed in the Supporting Information): residues Gly262, Lys263, and Trp266 in the helix αH (p66 thumb subdomain) that is involved into the primer–template binding, and Met230 and Gly231, two critical residues in the β12–β13 hairpin of the p66 palm subdomain that forms the "DNA primer grip" and helps the correct positioning of the 3′-OH end of the primer strand in the polymerase active site. In addition, DAVP-1 also contacts residues Met184 and Asp186 (within 3.5 to 4.0 Å) from the catalytically crucial YMDD motif of the palm subdomain. This new binding site further supports the nonclassical competitive inhibition of DAVP-1 and is fully consistent with its behavior distinctive from that of TNK-651.[4,5] Notably, the stacking of DAVP-1 onto Trp266 induces a conformational change of this residue relative to other related RT structures (Figure 2). Interestingly, Trp266, as well as all residues surrounding the drug binding pocket, belong to a highly conserved region of the HIV-1 RT from naive and drug-treated patients,[9] indicating that DAVP-1 interacts with amino acids that are not prone to mutations in presence of NNRTIs or NRTIs.

Another characteristic of the RT/DAVP-1 structure is that the protein conformation differs from that in RT/NNRTI complexes: the p66 thumb subdomain is folded into the

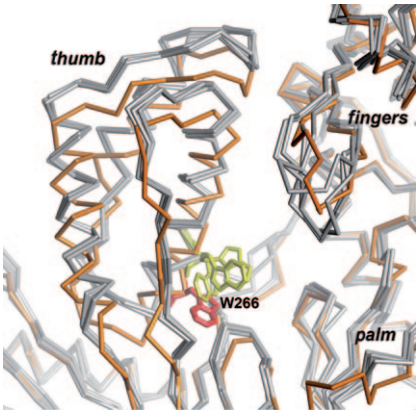

Figure 2. Detailed view around the NcRTI binding pocket showing a superposition of HIV-1 RT structures (in gray; PDB 1DLO, 2IAJ, 1QE1, and 1HQE) in the absence of NNRTI and in the RT/DAVP-1 complex (in orange). Residue W266 is shown in red in the present structure and in yellow in other RT structures.

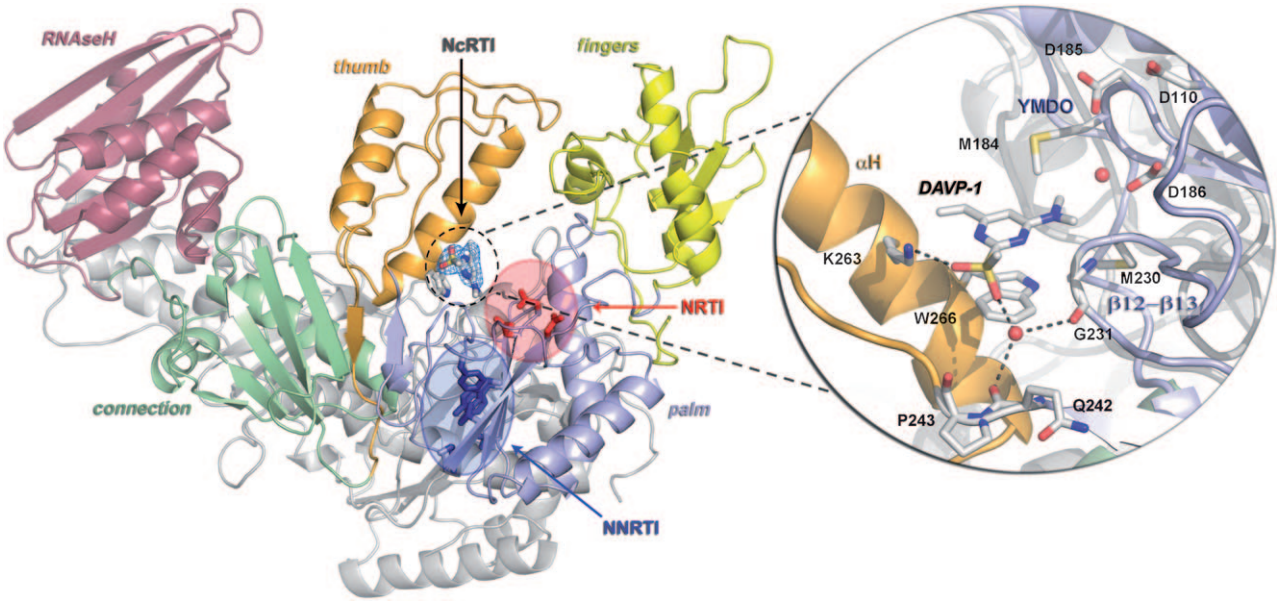

Figure 1. View of the HIV-1 RT/DAVP-1 complex, showing the NcRTI binding site and the relative position of binding sites for NRTIs (in a red shaded circle; the catalytic D110, D185, and D186 are represented as red rods) and NNRTIs (in a blue shaded circle; important residues of the NNIBP are represented as blue rods). The RT p51 subunit is shown in gray and the p66 subdomains (thumb, fingers, palm, connection, and RNAseH) are color coded. DAVP-1 and residue W266 are shown as rods. The electron density map is shown in blue around DAVP-1. The inset shows a detailed view of DAVP-1 within the binding pocket. For clarity, only some of the surrounding residues and two water molecules (red spheres) are depicted. Hydrogen bonds are represented with black dotted lines. Helix αH, the YMDD loop, and the β12–β13 hairpin are also labeled.

DNA-binding cleft, whereas it is in a hyperextended "open" conformation in RT/NNRTI crystal structures (for a review, see Ref. [10]). The protein structure is therefore analogous to the "closed" conformation observed in unligated RTs[11–13] or in RT bound to ATP.[8] However, significant differences are observed in the RT/NcRTI complex compared to "closed" conformations reported previously: a 3.0 Å translation of the p66 thumb subdomain towards the p66 palm subdomain is induced following the DAVP-1 binding (Figure 2). Excluding the p66 thumb and palm subdomains, the rest of the protein remains unaffected by the inhibitor binding. The significance of this conformational change is supported by the fact that it is observed in our two crystal forms obtained in presence of DAVP-1, whereas a classical conformation of the protein was obtained in a control crystallization experiment without NcRTI (see the Supporting Information).

A recent study showed that the Met184Val mutation induces partial resistance to INDOPY-1.[3] This residue appears in the neighborhood of DAVP-1 in our structure, and it is therefore possible, as expected from their similar inhibition mechanism, that the binding sites of DAVP-1 and INDOPY-1 at least partially overlap. It is also interesting to note that DAVP-1 analogues bearing bulkier groups in positions C4 and C5 (close to Met184) of the pyrimidine scaffold showed a decrease in or a complete loss of activity.[5]

To try to rationalize the biological data for our DAVP derivatives, we used the present crystal structure in modeling studies.[14] Molecular docking calculations and molecular interaction fields (MIFs) analysis were performed to investigate the binding mode and the activity determinants of compounds DAVP-2 and DAVP-3, which showed the same mechanism of action as DAVP-1. Structural water molecules (hereafter called W1 and W2) have been included in all the calculations, making it possible to reproduce the experimental binding conformation of the complex RT/DAVP-1 with a low ligand rmsd.[15] Docking calculations for DAVP-2 and DAVP-3 showed fundamental stacking interactions of these compounds with Trp266, even if in different orientation than for DAVP-1, which may justify their decreased affinity for this binding site (see Figure 9 in the Supporting Information). DAVP-2 loses hydrogen-bond contacts between the sulfone group, Lys263, and W2, while the diethylamino group is exposed to water and no longer involved in very favorable lipophilic interactions within the pocket lined by Met184 and Asp186 (GRID minimum point for CH_3 probe -4.5 kcal mol^{-1}). The latter interaction is also lost for DAVP-3, which, however, establishes profitable hydrogen-bond contacts between its *p*-methoxy group and the protonated N^{ε} of Lys263 and Lys259. These additional interactions can justify the improved activity of DAVP-3 with respect to DAVP-2.[5]

However, based on the present crystal structure, it remains unclear why a loss of activity of DAVP-1 was observed with the NNRTIs-resistant mutants Lys103Asn and Tyr181Ile. A possible explanation may be found in the structure of two unusual RT/NNRTIs complexes: RT/CP-94,707[16] and RT/DHBNH[17] (Figure 3). Interestingly, the side chains of Tyr181 and Tyr188 within these two crystal structures are in the conformation seen in the unligated RT and in the RT/DAVP-1 complex. In addition, both inhibitors

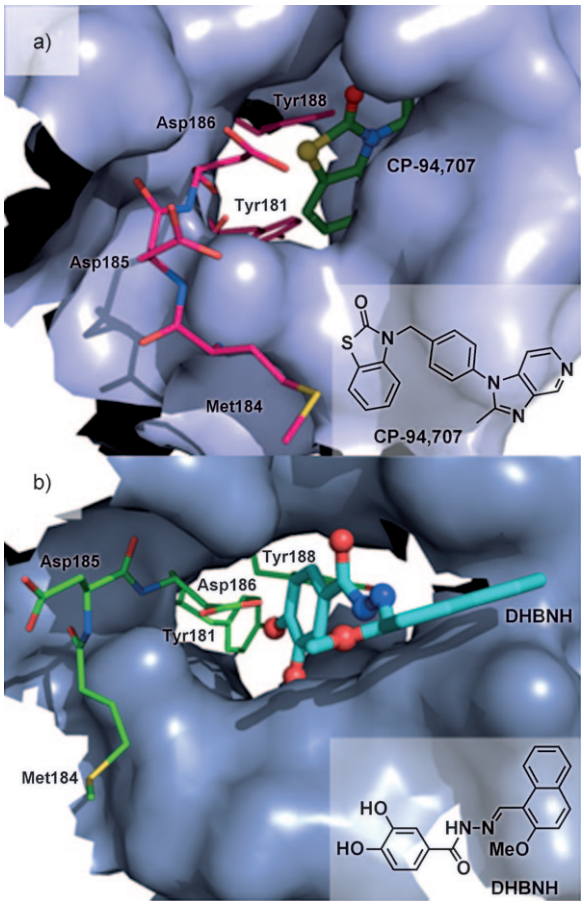

Figure 3. X-ray structures of two unusual NNRTI/RT complexes. For clarity only important residues of the NNIBP and catalytic site are shown. An opening between the NNIBP and the catalytic site can be ascertained. a) Structure of the CP-94,707/RT complex (PDB 1TV6). b) Structure of the DHBNH/RT complex (PDB 2I5J).

are directly involved in the formation of a connection tunnel between the NNIBP and the catalytic site defined by residues Tyr181 and Trp229 on opposite sides. Since DAVP-1 showed a drop in activity against those mutations that lie at the entrance site of common NNRTIs (close to Lys103) and at the edge of the above-mentioned connection tunnel (close to Tyr181), it seems reasonable to hypothesize that DAVP-1, owing also to its small size, could travel between the non-nucleoside- and nucleoside-binding pockets depending on which enzymatic form of RT it binds. However, this fascinating hypothesis needs to be explored further with additional crystallographic, biological, and molecular modeling studies.

Previous studies showed that DAVP-1 was able to inhibit HIV-1 RT by a competitive mechanism with the nucleotide substrate,[4] making this compound the second member of the newly discovered class of nucleotide-competing RT inhibitors (NcRTI) along with INDOPY-1. Our crystal structure discloses a new binding site for the NcRTI DAVP-1, located near the polymerization active site. These results provide the first structural basis for understanding the original mechanism of action of this NcRTI and will assist efforts to develop this new class of inhibitors. Further developments include the structure determination of NcRTIs in complex with the RT bound to a

DNA primer/template complex that is needed to obtain a complete view of the NcRTIs mechanism of action.

Received: October 8, 2009
Revised: November 24, 2009
Published online: February 4, 2010

Keywords: competitive inhibitors · enzyme models · HIV-1 reverse transcriptase · molecular modeling · structure elucidation

[1] Z. Zhang, M. Walker, W. Xu, J. H. Shim, J. L. Girardet, R. K. Hamatake, Z. Hong, *Antimicrob. Agents Chemother.* **2006**, *50*, 2772.
[2] M. Ehteshami, B. J. Scarth, E. P. Tchesnokov, C. Dash, S. F. Le Grice, S. Hallenberger, D. Jochmans, M. Gotte, *J. Biol. Chem.* **2008**, *283*, 29904.
[3] D. Jochmans, J. Deval, B. Kesteleyn, H. Van Marck, E. Bettens, I. De Baere, P. Dehertogh, T. Ivens, M. Van Ginderen, B. Van Schoubroeck, M. Ehteshami, P. Wigerinck, M. Gotte, K. Hertogs, *J. Virol.* **2006**, *80*, 12283.
[4] G. Maga, M. Radi, S. Zanoli, F. Manetti, R. Cancio, U. Hubscher, S. Spadari, C. Falciani, M. Terrazas, J. Vilarrasa, M. Botta, *Angew. Chem.* **2007**, *119*, 1842; *Angew. Chem. Int. Ed.* **2007**, *46*, 1810.
[5] M. Radi, C. Falciani, L. Contemori, E. Petricci, G. Maga, A. Samuele, S. Zanoli, M. Terrazas, M. Castria, A. Togninelli, J. A. Este, I. Clotet-Codina, M. Armand-Ugon, M. Botta, *ChemMedChem* **2008**, *3*, 573.
[6] D. Jochmans, *Virus Res.* **2008**, *134*, 171.
[7] A. L. Hopkins, J. Ren, R. M. Esnouf, B. E. Willcox, E. Y. Jones, C. Ross, T. Miyasaka, R. T. Walker, H. Tanaka, D. K. Stammers, D. I. Stuart, *J. Med. Chem.* **1996**, *39*, 1589.
[8] K. Das, S. G. Sarafianos, A. D. Clark, Jr., P. L. Boyer, S. H. Hughes, E. Arnold, *J. Mol. Biol.* **2007**, *365*, 77.
[9] F. Ceccherini-Silberstein, F. Gago, M. Santoro, C. Gori, V. Svicher, F. Rodriguez-Barrios, R. d'Arrigo, M. Ciccozzi, A. Bertoli, A. d'Arminio Monforte, J. Balzarini, A. Antinori, C. F. Perno, *J. Virol.* **2005**, *79*, 10718.
[10] S. G. Sarafianos, B. Marchand, K. Das, D. M. Himmel, M. A. Parniak, S. H. Hughes, E. Arnold, *J. Mol. Biol.* **2009**, *385*, 693.
[11] Y. Hsiou, J. Ding, K. Das, A. D. Clark, Jr., P. L. Boyer, P. Lewi, P. A. Janssen, J. P. Kleim, M. Rosner, S. H. Hughes, E. Arnold, *J. Mol. Biol.* **2001**, *309*, 437.
[12] Y. Hsiou, J. Ding, K. Das, A. D. Clark, Jr., S. H. Hughes, E. Arnold, *Structure* **1996**, *4*, 853.
[13] S. G. Sarafianos, K. Das, A. D. Clark, Jr., J. Ding, P. L. Boyer, S. H. Hughes, E. Arnold, *Proc. Natl. Acad. Sci. USA* **1999**, *96*, 10027.
[14] Details of the molecular modeling calculations are reported in the Supporting Information.
[15] Calculation of molecular interaction fields (MIFs) by GRID software using the water probe (OH2) revealed two minima (-8.9 and -7.6 kcal mol^{-1}) located exactly where W1 and W2 were found in the X-ray structure.
[16] J. D. Pata, W. G. Stirtan, S. W. Goldstein, T. A. Steitz, *Proc. Natl. Acad. Sci. USA* **2004**, *101*, 10548.
[17] D. M. Himmel, S. G. Sarafianos, S. Dharmasena, M. M. Hossain, K. McCoy-Simandle, T. Ilina, A. D. Clark, Jr., J. L. Knight, J. G. Julias, P. K. Clark, K. Krogh-Jespersen, R. M. Levy, S. H. Hughes, M. A. Parniak, E. Arnold, *ACS Chem. Biol.* **2006**, *1*, 702.

